

# Analysis and Design of Wideband Passive UHF RFID Tags Using a Circuit Model

Daniel D. Deavours

**Abstract**—The great majority of commercial UHF RFID tags are based on dipole antennas using a modification of a T-match as a matching circuit. The literature contains examples of wideband matching, but provides little insight as to how wideband behavior is achieved. Here, we present a simple circuit-based theory to describe the antenna, matching circuit, and IC behavior; we present an approach for developing an impeding matching strategy to maximize bandwidth; and we present a concrete example and analysis using a method of moments (MoM) numerical solver. The results show very good agreement with theory.

## I. INTRODUCTION

A number of operating conditions around UHF RFID impose a relatively wide bandwidth requirement, including: electrically short antennas, a world-wide operating band from 860 to 960 MHz (perhaps including 840 MHz from a new operating band in China), as well as shifts in resonant frequency due to the affects of dielectric material. There is significant economic pressure to develop RFID tags that can operate over a large bandwidth, provide good performance, and are physically small. Obviously, these are conflicting requirements.

In this paper, we undertake the systematic analysis of the most common UHF RFID tag antenna and matching circuit designs. We then transform the common circuit representations into the canonical model of a two-stage bandpass filter. Given this new insight, we are able to synthesize a circuit model that maximizes a number of useful design objectives, especially bandwidth.

We illustrate the usefulness of this approach with five practical examples. These examples allow us to draw some useful conclusions. For example, we show that by properly designing the antenna to behave as a bandpass filter, we are able to achieve an improvement in bandwidth by a factor of approximately 3.3 over a more naive approach. The examples also show that the synthesized circuit model is an excellent predictor of what is realizable with realistic RFID tag designs. Finally, we show some theoretical results on item-level tags.

## II. BACKGROUND

### A. RFID Tag Design

Numerous papers have been written describing how to construct an antenna for RFID. A good survey can be found

This work is funded in part by the Information and Telecommunications Technology Center.

D. Deavours is with the Information and Telecommunications Technology Center, University of Kansas, Lawrence, KS 66045, USA. Email: deavours@ittc.ku.edu

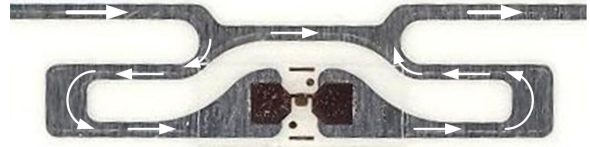


Fig. 1. Commercial tag matching circuit with superimposed currents.

here [1], and a more detailed account is given in [2].

Within the RFID industry, RFID antennas that have a length of approximately 92 mm are popular because of the convenience of placing tag within a 101.6 mm wide label. Note that half-wave dipole at 915 MHz has a length of 164 mm, so additional inductance must be added to the short antenna to make the antenna resonate at a lower frequency. Also, there are strong economic pressures on the price of the RFID tag antenna, so the width is also minimized. Widths of 8 mm are common, though narrower and considerably wider widths are commercially available. Note that this relatively long, narrow, short dipole has a significantly higher  $Q$  than a traditional half-wave dipole.

To aggravate these constraints, the world-wide frequency range of UHF RFID tags are defined between 860–960 MHz [3], and placing tags on a dielectric material can change the resonant frequency of the tag / antenna. Maximizing bandwidth becomes a primary performance constraint.

### B. Circuit Models

Part of the problem involves accurately modeling the matching circuit of an RFID tag. Fig. 1 shows a typical matching circuit for a commercial RFID tag with superimposed currents. We can see that there are inductive elements and likely considerable coupling between the various elements. In [4], the circuit diagram shown in Fig. 2 is proposed as an equivalent circuit for the RFID tag, though the matching circuit considered in [4] was simpler than the one shown in Fig. 1, which is more common. In [5], the circuit shown in Fig. 3 is presented as a more general model to address the complexities of the circuit shown in Fig. 1.

We note that the circuit in Fig. 3 can be fairly closely mapped to the traces in Fig. 1, but in Fig. 3, inductive coupling between elements is neglected. From [4], for example, we can assume that there is inductive coupling between  $L_{series}$  and  $L_{shunt}$  and possibly between  $L_{ant}$ . Fortunately, any inductive coupling will serve to transform the antenna impedance, and will not for example disturb the antenna  $Q$  or resonant frequency. Thus, we can conclude that Fig. 3

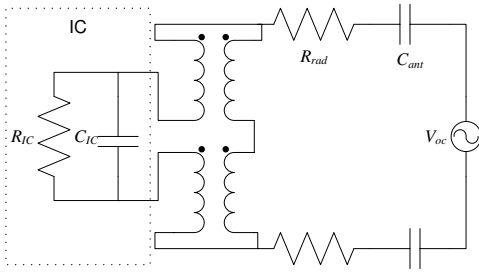


Fig. 2. Circuit model from [4].

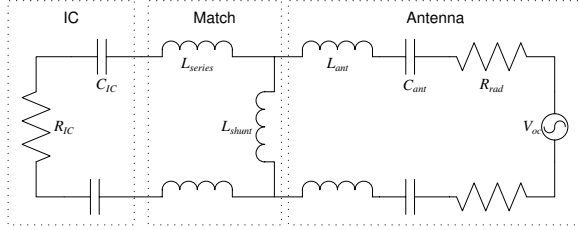


Fig. 3. Circuit model from [5].

is qualitatively correct, though an exact translation between circuit element values and physical geometry is lost. We will return to this point below.

The complex power wave reflection coefficient is given as [6]

$$s = \frac{Z_c - Z_a^*}{Z_c + Z_a}.$$

The power reflection coefficient is  $|s|^2$ , return loss is then  $20 \log |s|$ , and the power transfer efficiency is  $1 - |s|^2$ .

### C. Bandwidth

There has been relatively little systematic study of the methodology of maximizing bandwidth, though there has been some effort. Rao et al. [2] lays out foundational theory for RFID antennas and tag measurement, but offers only a simplistic antenna design methodology. Chau et al. [7] addresses bandwidth directly, but largely neglects the role of impedance matching. Cho et al. [8] illustrates a tag with a 8.5% bandwidth, but the dimensions were found using genetic algorithms and thus provide little insight. Chang and Lo [9] show how to use a capacitively loaded matching circuit to achieve broadband behavior, but provide no theoretical analysis.

The most relevant work we are aware of is Son and Pyo [10], which shows a methodology restricted to inductively-coupled feeds and assumes a constant IC impedance. The IC impedance is often modeled as a parallel RC circuit [11], [12] and thus changes with frequency. In this paper, we relax both assumptions of [10], expand the circuit model to the most commonly used matching circuit, and apply it to five practical examples.

## III. TRANSFORMATION

### A. Circuit Model

For simplicity, we use a series RLC circuit model to model the antenna. The series RLC model is remarkably

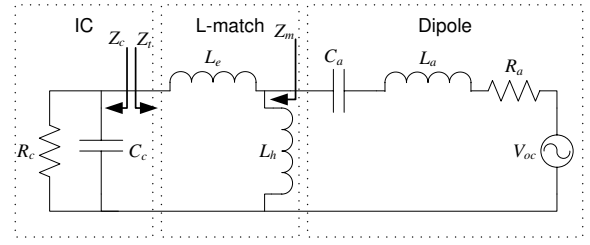


Fig. 4. Complete circuit model of RFID tag, matching circuit, and IC.

accurate for modeling the reactance of a narrow dipole antenna near resonance over a relatively small frequency range, but the constant resistance assumption is flawed, especially for electrically short (high Q) dipole antennas. A more accurate 4- and 5-element circuit models are available [13], [14], but add additional complexity to the analysis. For now, we simply note the model deficiency and proceed with the simpler circuit model.

A series RLC circuit can obviously be described by the circuit parameters  $R$ ,  $L$ , and  $C$ , but it can also be uniquely specified from  $R$ , the resonant frequency  $\omega_0$ , and the quality factor  $Q_s$ . The relationship between these is well known:

$$\begin{aligned} \omega_0 &= \frac{1}{\sqrt{LC}} \\ Q_s &= \frac{\omega_0 L}{R} = \frac{1}{\omega_0 RC} \end{aligned}$$

Let  $R_c$  and  $C_c$  denote the IC (“chip”) resistor and capacitor respectively; the parallel combination of  $R_c$  and  $C_c$  model the IC impedance. The impedance of the IC can be computed:  $Z_c = (1/R_c + j\omega C_c)^{-1}$ . If  $Z_c = R + jX$ , then we can define the quality factor of the IC as  $Q_c = X/R = \omega R_c C_c$ .

While numerous novel antenna models have been proposed in the literature, the great number of antennas use a simple variant of the T-match [1] originally proposed by Uda [15]. Here, we deviate from Uda’s classic analysis using even-odd mode analysis, and instead focus on a circuits-based approach. We take Fig. 3 as a starting point for our analysis. For simplicity, we reduce the balanced circuit into an unbalanced equivalent circuit shown in Fig. 4.

### B. Circuit Transformation

We observe that the circuit presented in Fig. 4 is complete and reasonably accurate, but cumbersome. Here, we will transform the circuit into a more useful form. Consider a circuit given in 5(a). Here, we will use an identity in which the shunt-series inductors are replaced with a series-shunt inductor with a scaled load impedance.

Let:

$$\begin{aligned} \alpha &= \frac{L_h}{L_e + L_h} \\ Z_L^* &= \alpha^2 Z_L \\ L_n &= \alpha^2 (L_e + L_h) \\ L_{se} &= \frac{L_e L_h}{L_e + L_h} \end{aligned}$$

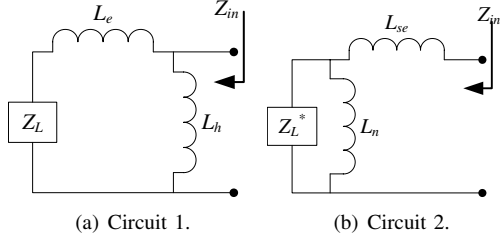


Fig. 5. L-match transform identity.

The theorem states that Circuits 1 and 2 present identical impedances. The proof is simple enough that we present it here.

$$\begin{aligned}
Z_{in} &= \frac{Z_L^* X_n}{Z_L^* + X_n} + X_{se} \\
&= \frac{\alpha^2 Z_L \alpha^2 (X_e + X_h)}{\alpha^2 Z_L + \alpha^2 X_m} + \frac{X_e X_h}{X_e + X_h} \\
&= \frac{\alpha^2 Z_L X_m}{Z_L + X_m} + \frac{X_e X_h}{X_e + X_h} \\
&= \frac{X_h^2}{X_m^2} \frac{Z_L X_m}{Z_L + X_m} + \frac{X_e X_h}{X_e + X_h} \\
&= \frac{X_h^2 Z_L}{X_m (Z_L + X_m)} + \frac{X_e X_h}{X_m} \\
&= \frac{Z_L X_h^2}{X_m (Z_L + X_m)} + \frac{X_e X_h}{X_m} \frac{Z_L + X_m}{Z_L + X_m} \\
&= \frac{Z_L X_h^2 + Z_L X_e X_h + X_e X_h X_m}{X_m (L_L + X_m)} \\
&= \frac{Z_L X_h (X_e + X_h) + X_e X_h (X_e + X_h)}{(X_e + X_h)(Z_L + X_e + X_h)} \\
&= \frac{Z_L X_h + X_e X_h}{Z_L + X_e + X_h}
\end{aligned}$$

We can now perform the above general transformation on the specific circuit shown in Fig. 4. Specifically, let:

$$\begin{aligned}
R_n &= \alpha^2 R_c \\
C_n &= \frac{C_c}{\alpha^2} = \frac{Q_m}{\omega_0 R_n} \\
L_n &= \alpha^2 L_m = \frac{R_n}{\omega_0 Q_m} \\
L_{se} &= \frac{L_e L_h}{L_e + L_h}
\end{aligned}$$

Then, if we combine  $L_{se}$  with  $L_a$ , the resulting circuit is shown in Fig. 6. The result of this transformation is a circuit that is in the canonical form of a two-stage bandpass filter.

### C. Synthesis

The practical implication of this circuit model, as we demonstrate in the following section, is that we can synthesize a desired bandpass circuit model, and once the circuit model is carefully tuned, it is straightforward to fabricate an antenna and matching circuit that presents a nearly-identical impedance. And again, because the circuit is simple, it is straightforward to synthesize a circuit given

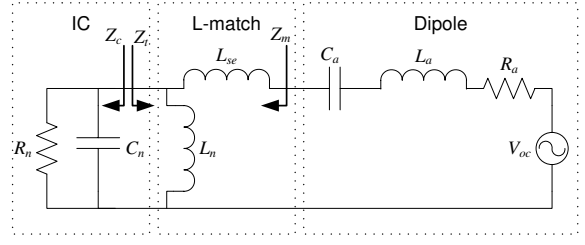


Fig. 6. Combined equivalent circuit.

certain parameters. Thus, the design process may be fairly automated.

We assume that the design parameters that are given are the form factor and the IC. The form factor largely determines  $Q_a$  and  $R_a$ , and of course the IC prescribes  $R_c$  and  $C_c$ . To maximize bandwidth, one should select the resonant frequency of the series and parallel RLC circuits of Fig. 6 to be the same and equal to the geometric mean of the band.

The remaining parameter to “tune” is  $\alpha$ , but notice that any change in  $\alpha$  will also change  $L_{se}$  and thus the series RLC resonance. If one wishes to change  $\alpha$ , one will also need to modify  $\omega_a$ , the resonant frequency of the antenna, so that the resonant frequency of the series RLC circuit remains  $\omega_0$ . Below, we show how to synthesize  $\omega_a$ ,  $L_a$ , and  $C_a$  in terms of  $Q_a$ ,  $R_a$ ,  $L_{se}$ ,  $\omega_0$ , and  $\alpha$ .

Recall the resonant frequency of the series RLC circuit is

$$\omega_0^2 = \frac{1}{C_a (L_a + L_{se})},$$

which we rearrange as

$$\omega_0^2 L_a C_a + \omega_0^2 L_{se} C_a - 1 = 0.$$

Using identities for  $L_a$  and  $C_a$  and canceling, we can rewrite

$$\frac{\omega_0^2}{\omega_a^2} + \frac{\omega_0^2 L_{se}}{\omega_a R_a Q_a} - 1 = 0,$$

and finally

$$\omega_a^2 - \omega_a \frac{\omega_0^2 L_{se}}{R_a Q_a} - \omega_0^2 = 0.$$

One can see this is a quadratic in  $\omega_a$  and can solve in the normal way. Once  $\omega_a$  is known, it is straightforward to compute the circuit parameters.

We find it algebraically simpler to solve in terms of  $L_a$ . We know that  $C_a = \frac{L_a}{(Q_a R_a)^2}$ . Starting from

$$\begin{aligned}
\omega_0^2 L_a C_a + \omega_0^2 L_{se} C_a - 1 &= 0, \\
\frac{\omega_0^2 L_a^2}{(R_a Q_a)^2} + \frac{\omega_0^2 L_{se} L_a}{(R_a Q_a)^2} - 1 &= 0, \\
L_a^2 + L_a L_{se} - \left( \frac{Q_a R_a}{\omega_0} \right)^2 &= 0.
\end{aligned}$$

Now, we can apply the quadratic equation and consider only positive inductances to find

$$L_a = \frac{\sqrt{L_{se}^2 + \left( \frac{2 R_a Q_a}{\omega_0} \right)^2} - L_{se}}{2}.$$

An alternative derivation shows an equivalent expression in a different form:

$$L_a = \sqrt{\left(\frac{R_a Q_a}{\omega_0}\right)^2 + \left(\frac{(1-\alpha)(L_e + L_h)}{2\sqrt{2}}\right)^2} - \frac{1-\alpha}{2\sqrt{2}}(L_e + L_h).$$

Two comments about application of this in practice. First, the circuit model that this is based upon ignores inductive coupling, i.e., the transformer in Fig 2. Generally, computing the amount of coupling is difficult. Inductive coupling will not change  $Q_a$  or  $\omega_0$  of the circuit, only  $R_a$ , so if one is able to estimate the degree of coupling, one can simply scale  $R_a$  accordingly, and the rest of the analysis will follow without modification. With a transformed  $R_a$ , the appropriate value of  $\alpha$  can be computed, and the circuit elements are synthesized according to the equations given above.

Second, we notice that  $L_{se}$  is the parallel combination of  $L_e$  and  $L_h$ , and if  $\alpha$  is close to zero (which is common because  $R_c$  is normally much larger than  $R_a$ ), then  $L_{se}$  is small, especially compared to  $L_a$  for most antennas with relatively large  $Q_a$ . As a practical matter, one can assume  $L_{se}$  is zero, assume  $\omega_a = \omega_0$ , and then manually adjust the inductance of the antenna and matching circuit to achieve the desired impedance behavior.

Next, we consider heuristics for estimating the circuit parameters of a dipole from its geometry. From [16] we know

$$R_a = 80\pi^2\beta^2 \left(\frac{l}{\lambda}\right),$$

where  $0.5 \leq \beta \leq 1$  depending on how the current is distributed along the antenna, and  $l$  is the length of the antenna. For  $\beta = 0.7$ , we would estimate a 92 mm long dipole antenna would have  $R_a = 30$  Ohms. A meander-line geometry is used to create a compact geometry, and create a sufficiently large  $L_a$  so the antenna will resonate despite being electrically short. A smaller antenna will usually have a larger  $Q_a$ , so the physical size can be used to adjust  $Q_a$ . Estimating inductance and capacitance values for dipoles with meandering geometries is challenging and outside the scope of this paper.

Constructing inductances from distributed traces is particularly troublesome, since it is not clear whether inductance can be defined for anything but a closed loop. However, using [17], we can estimate that inductance of a trace with length  $l$ , width  $w$ , and thickness  $t$ , all units in cm, can be estimated as follows.

$$L = 0.002l \left( \ln \frac{l}{w+t} + 1.193 + 0.2235 \frac{w+t}{l} \right) (nH)$$

#### IV. EXAMPLES

In this section, we present theoretical and practical results for several examples that represent “real-world” challenges for RFID tags, and show how this technique can be used to maximize performance.

Normally, circuits are used to model complex antenna geometries as useful abstractions, and it is not straightforward

to synthesize a geometry from a circuit description. Much of what we do in this section is done manually. We emphasize that there relationships between the two, the details of which are outside the scope of this paper, but that insight and tools to manipulate the circuit-equivalent of the antenna can be used to guide the antenna design process.

##### A. Broader Bandwidth Antenna

Because of the different frequency bands used world-wide and because dielectric materials can shift the resonant frequency of the antenna, bandwidth becomes one of the primary constraints. Here, we consider an antenna with  $Q_a = 15$ , which is approximately that of a meandering dipole with a length of 92 mm and a width of 8 mm. This size was selected because it is popular in the high volume commercial market, and thus conclusions we can draw from this example are of commercial relevance. For this antenna, we let  $R_a = 30$  Ohms, typical of a 92 mm antenna. Further, assume the use of an IC with  $R_c = 1500$  Ohms and  $C_c = 1.2$  pF for a  $Q_c = 10$ . The question sought here is whether one can achieve world-wide operation and maintain a 10 dB return loss (or, stated equivalently, an 90% power transfer efficiency) with those constraints, and the benefit that one would achieve using this technique as opposed to a more naive approach.

First, we take the Gen 2 standard definition of world-wide operation to be between 860 and 960 MHz, with the geometric mean of 908.6 MHz. The return loss of 10 dB specifies a reflection coefficient of 0.3612 in the center of the band, which can be achieved if  $R_n = 55.9$  Ohms, which implies that  $\alpha = 0.1930$ . To cancel  $C_c$ ,  $L_e + L_h = 25.57$  nH, so  $L_e = 20.63$  nH and  $L_h = 4.94$  nH. The inductance of the antenna is calculated to be 76.86 nH and the resonant frequency of 931.9 MHz to achieve  $Q_a = 15$  and  $R_a = 30$ .

Next, to verify the validity of the circuit model, we developed an antenna to provide an impedance that is similar to that of the synthesized circuit. The geometry is given in Fig. 7(a). One can see that the antenna requires a considerable amount of meandering to achieve resonance. Also, a portion of the matching circuit slightly exceeds the self-imposed 8 mm width; this can be rectified with additional design work and is not critical for this discussion.

For comparison, we also include a “naive” tag design in Fig. 7(b) that is electrically short (i.e., resonates at a much higher frequency) but designed to present a conjugate impedance match at 915 MHz. The naive antenna has a resonant frequency of about 1011 MHz. Estimating  $Q_a$  at 915 (off resonance) using  $\frac{\omega}{2R} \frac{dX}{d\omega}$ , we find  $Q_a = 14.3$ . The antenna impedance (without matching circuit)  $Z_a$  at 915 MHz was found to be  $29.5 - j88.8$  Ohms. Other circuit values are presented and compared in Tab. I. Notice that  $Q_a$  for the naive tag is very close to  $Q_a$  for the wideband tag, so the matching circuit is clearly extending the bandwidth of the tag.

Next, we analyze both the circuit and the simulated tag antenna design. We consider the impedance looking into the antenna from the IC, or  $Z_t$  from Fig. 4. The antenna was

TABLE I  
SUMMARY OF CIRCUIT PARAMETERS FOR EXAMPLE TAGS.

	$Q_a$	$R_a$	$f_a$ (MHz)	$L_e$	$L_h$	$\alpha$
Wideband	15.0	30.0	932	20.63	4.94	0.193
Naive	14.3	29.5	1056	11.73	8.92	0.432

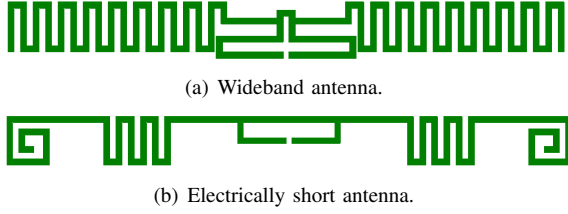


Fig. 7. Geometry of (a) a wideband and (b) naive narrowband RFID tag.

simulated using a method of moments (MoM) code. Plotted in Fig. 8 is the circuit impedance, the simulated antenna impedance, and the conjugate IC impedance. One can see excellent agreement between the circuit model and simulated antenna.

Finally, we calculate the return loss of the circuit, and plot the results in Fig. 9. We see that the antenna does not achieve the 10 dB return loss over the entire 860–960 MHz band. However, if one only considers 865–955 MHz, which covers the practical band of world-wide operation, we see that it does in fact meet the 10 dB return loss. Again, the return loss shows excellent agreement between the circuit and simulated antenna. For comparison, we include the return loss of the naive design, which shows much more narrowband behavior and provides only 27 MHz of 10 dB return loss. This suggests an improvement in bandwidth by a factor of about 3.3 using the proposed technique.

Obviously, one can achieve much better return loss over a narrower frequency band. For example, a return loss of 14 dB can be achieved between 865 and 930 MHz (covering the vast majority of world-wide operation, including North America and Europe) using the proposed approach.

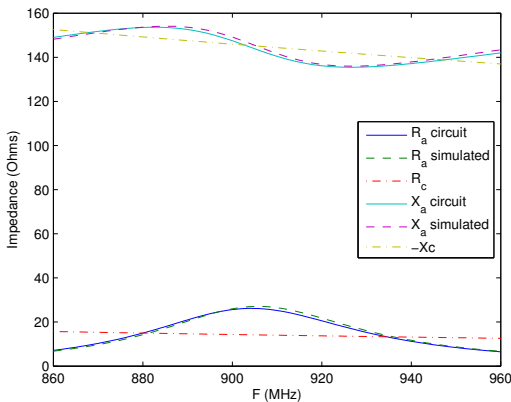


Fig. 8. Example 1: Impedance vs. frequency for the circuit model, simulated antenna, and IC. (Inductive coupling not shown.)

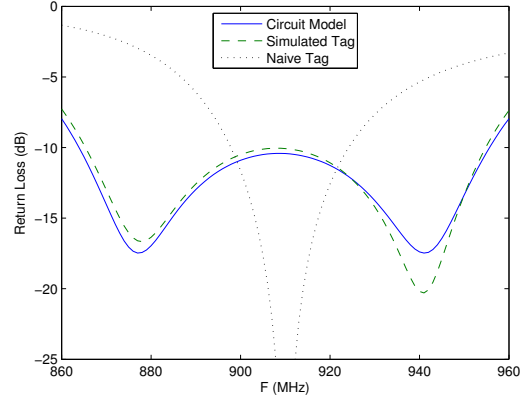


Fig. 9. Example 1: Return loss vs. frequency.



Fig. 10. Tag geometry that implements Example 2.

### B. Example 2: Dual-Matched Tag for Frequency Diversity

Next, we consider a use case in which the RFID tag must operate in at 915 MHz for normal RFID operation, but must also operate at 1.1 GHz band for other (proprietary) operation. Providing continuous operation efficiently over the entire band is not possible, but it is possible to provide impedance matching at the two different frequency bands. For this example, we assume  $R_c = 1500$  Ohms and  $C_c = 1.2$  pF for a  $Q_c = 11.4$  at 1 GHz. A similar use case may be smaller RFID tag required to operate at 840 MHz in China and 955 MHz in Japan.

To solve this problem, we simply create a bandpass filter centered at 1 GHz and impose a large ripple in the center of the band. The return loss is set to approximately 2.5 dB at 1 GHz, which is very poor, but does provide good return loss at 915 and 1105 MHz. Circuit values are:  $R_a = 30$  Ohms,  $L_a = 68.82$  nH,  $C_a = .3399$  pF,  $\alpha = .3741$ ,  $L_e = 13.07$  nH,  $L_h = 7.810$  nH.

An antenna was designed to match these circuit values and is presented in Fig. 10. As before, we show the circuit impedance and the simulated tag impedance  $Z_t$  in Fig. 11. We note that  $Z_t$  for the circuit and simulated tag show good agreement, considering the relatively wide bandwidth considered here, in which the dipole resistance can change significantly over the band. With some additional design work, one may achieve an even closer match to the circuit impedance. However, the desired return loss was achieved, which is shown and compared to the circuit return loss in Fig. 12.

We can also compare the 10 dB return loss from this tag to the wideband tag presented in Fig. 7. Here, the tag presents a 10 dB return loss bandwidth of 26 MHz, which is consistent with the 27 MHz of Fig. 7(b).

Note that while there are relatively few use cases in which

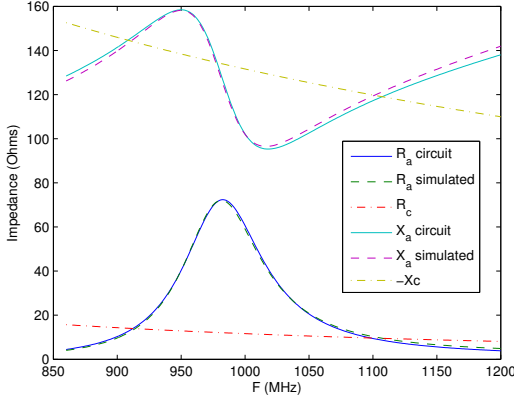


Fig. 11. Example 2: Impedance vs. frequency for the circuit model, simulated antenna, and IC.

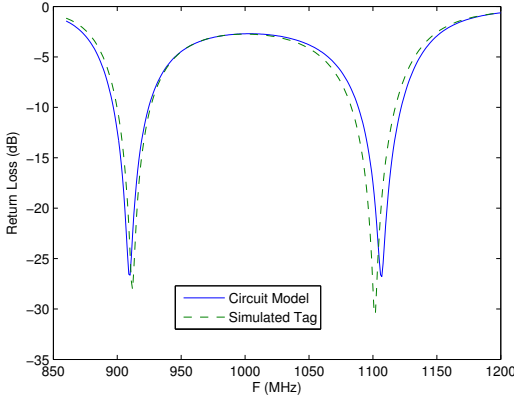


Fig. 12. Example 2: Return loss vs. frequency.

RFID tags are required to operate at both 915 and 1.1 GHz, it is common to encapsulate RFID tags in some dielectric material, such as a plastic or ceramic. This case is considered next.

### C. Example 3: Dual-Matched Tag for Dielectric Diversity

Surrounding the tag with a dielectric material has the affect of reducing the resonant frequency of the antenna, similar to the previous example, except the dielectric does not change the impedance of the IC. One would like to be able to verify the quality of a tag in free space before encapsulation, and perhaps use the same antenna without encapsulation for other purposes, so it is desired to have good operation of the tag both in free space and when encapsulated. In this example, we exercise the ability to use the same circuit theory to construct a tag that operates efficiently at 915 MHz in free space, but also operates efficiently when encapsulated in a dielectric material that has the effect of reducing the resonant frequency of the antenna by about 0.81. We continue to assume a physical size constraint of 92 by 8 mm. We also assume that the IC impedance is  $11.5 - j131$  Ohms at 915 MHz.

To address this set of constraints, we replace the IC with a



Fig. 13. Tag geometry that implements Example 3.

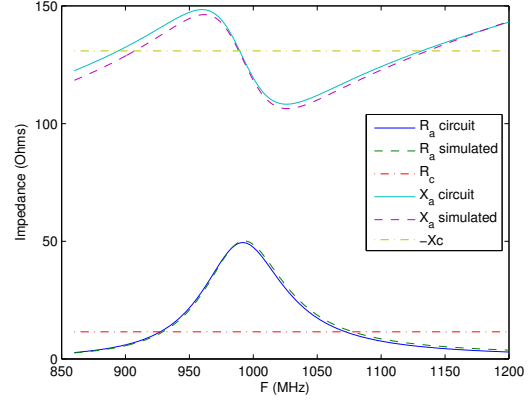


Fig. 14. Example 3: Impedance vs. frequency for the circuit model, simulated antenna, and IC.

constant series impedance of  $11.5 - j131$  Ohms. As before, we set the resonant frequency of the series RLC circuit to be 1 GHz (the antenna resonance is 1045 MHz), and to cancel the IC reactance at resonance,  $L_e + L_h = 20.88$  nH. Note that the higher resonance of the antenna where the same physical size is electrically larger compared to a wavelength at 1 GHz, so  $Q_a$  is smaller, or approximately 12.

Next, we vary  $\alpha$  until we minimize the return loss at 915 MHz and at 1.1 GHz. We find this occurs with  $\alpha = 0.30$ , and thus  $L_e = 14.61$  nH and  $L_h = 6.26$  nH.

We modified the antenna from Fig. 10 to present a similar impedance to the synthesized circuit, which we show in Fig. 13. The impedance and return loss of the circuit and simulated tag antenna are shown in Figs. 14 and 15. We note that the tag is able to very closely match the circuit resistance, but the reactance seems to diverge slightly over the band, illustrating a limitation of the model. We again see excellent agreement between the predicted and achievable return loss.

We do note that, compared to Example 2, the achievable return loss is significantly worse at the two frequencies of interest. This is largely due to IC capacitance staying constant with frequency. This shows that the parallel IC capacitance is an important and useful component in broadband impedance matching. Improving in the return loss shown here will likely require a modification to the dipole, perhaps using reactive loading.

### D. Example 4: Small Item-Level Tag

Next, we examine this technique applied to item-level tagging. Item-level tags are very small, often less than 22 mm<sup>2</sup>, though some are larger, such as 47 by 42 mm, or 18 by 32 mm. The majority of item-level tag antennas in commercial use are electrically short, meaning that they

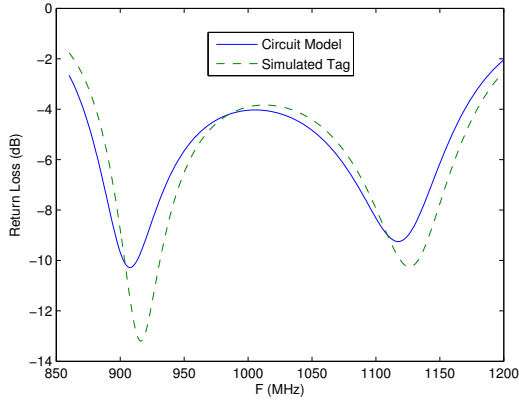


Fig. 15. Example 3: Return loss vs. frequency.

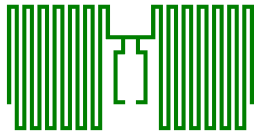


Fig. 16. Tag geometry that implements Example 4.

operate well below resonance. Creating an item-level tag with sufficient reactance can be a challenge, will require small feature sizes, and is likely to suffer from conductive losses.

Assume that we are prescribed an IC with  $R_c = 400$  Ohms and  $C_c = 2.2$  pF, yielding  $Q_c = 5$ . Also assume the size constraint is set to 32.5 mm by 16.5 mm, and the objective is to maximize the worst-case performance over the 900–930 MHz frequency band. From a preliminary design, we estimate  $Q_a = 97$  and  $R_a = 6.8$  Ohms. We then construct the circuit model and vary  $\alpha$  until we maximize the minimum return loss over the 900–930 MHz band. We found that this happens at  $\alpha = 0.2397$ , which yields a best return loss of 5.3 dB, and a worst return loss of 3.5 dB. This suggests that this sized geometry is capable of greater than 50% efficiency (ignoring conductive or dielectric losses).

As before, we show the antenna geometry that implements the circuit impedance in Fig. 13, the circuit and simulated tag impedance in Fig. 14, and the return loss calculated from the circuit and simulated antenna in Fig. 18. Again, the two show excellent agreement. We were able to rapidly vary the circuit model to find an optimum, then relatively easily construct a tag geometry to implement the circuit. Refinements in circuit parameters can readily be fed back into the circuit model to further improve performance.

We note that this tag is able to operate with better than 50% efficiency over the entire FCC band, and a peak of 70% efficiency, which means the theoretical read distance would be reduced between 16–30% (this neglects a likely reduction in antenna efficiency). What is compromised for bandwidth is the relatively large antenna impedance, which for many ICs will result in a small backscatter signal strength [18].

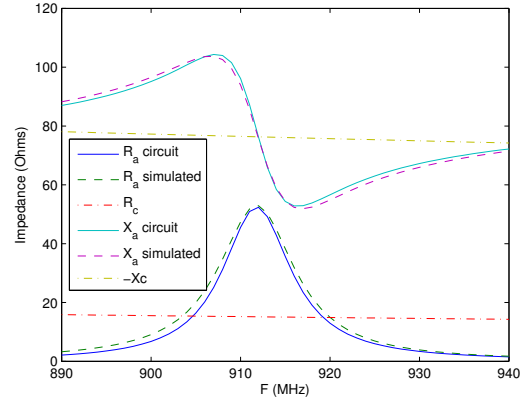


Fig. 17. Example 4: Impedance vs. frequency for the circuit model, simulated antenna, and IC.

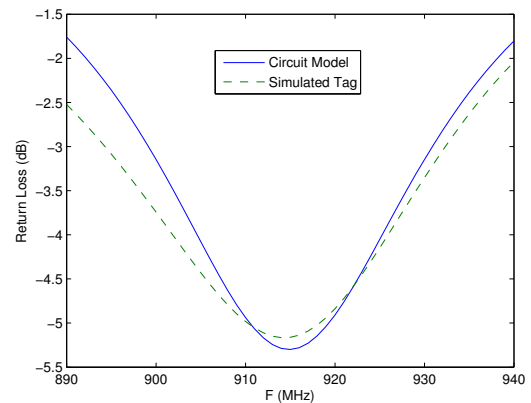


Fig. 18. Example 4: Return loss vs. frequency.

### E. Example 5: Smaller Item-Level Tag

Finally, we briefly consider an antenna that fits within a 22 by 22 mm form factor. A preliminary design shows an approximate  $Q_a = 187$  and  $R_a = 3$  Ohms. We varied  $\alpha$  until we maximize the worst-case performance over the band. We find this occurs with  $\alpha = 0.2182$  and  $R_n = 19.041$  Ohms. The large mismatch between antenna and IC impedance is likely to result in poor backscatter signal strength. However, the worst-case efficiency over band is 31.5%, which is quite poor, and will result in a reduction in read distance by nearly half. Given the small size of the tag, a 50% reduction in read distance is surprisingly good. For brevity, we omit a detailed analysis and comparison against a sample implementation.

## V. CONCLUSION

In this paper, we present a circuit model for the RFID tag antenna and IC, and show how through a simple transformation we can change the matching circuit from a series-shunt L-match to a shunt-series L-match. This allows us easily reformulate the tag antenna and matching circuit problem into a classical two-stage bandpass filter. Recognizing this, we can set bandpass parameters to maximize bandwidth or

any other metric. We see that the classic impedance matching problem is an under-constrained problem, and by carefully selecting the free parameters, we can control the impedance bandwidth behavior. Using this technique, we showed that we can improve bandwidth by a factor of approximately 3.3.

We consider a number of useful examples, and use a combination of quick preliminary simulation results to estimate  $Q_a$  and  $R_a$ , then use the circuit model to synthesize a near-optimum solution for each example. We then show that we are able to construct an RFID tag antenna and matching circuit that implements the circuit model quite accurately and over a variety of conditions.

From this, we can conclude that the circuit model is a remarkably accurate model that is useful for rapidly exploring the design space given a set of constraints. Once the desired circuit model is found, it is straightforward to construct an RFID tag antenna that closely matches the circuit model.

Finally, we applied this technique to a number of practical, “real world” problems, including a wideband RFID tag, two examples with impedance matching at two frequencies, and maximizing worst-case performance of small, “item-level” tags. We conclude that the bandpass filter model is an effective and useful tool for describing and designing wideband UHF RFID tags.

## VI. ACKNOWLEDGMENTS

The author would like to acknowledge Daniel Dobkin for help with the early manuscript, and the reviewers who made several helpful suggestions.

## REFERENCES

- [1] G. Marrocco, “The art of UHF RFID antenna design: impedance-matching and size-reduction techniques,” *IEEE Antennas and Propagation Magazine*, vol. 50, no. 1, pp. 66–79, Feb. 2008.
- [2] K. V. S. Rao, P. V. Nikitin, and S. F. Lam, “Antenna design for UHF RFID tags: A review and a practical application,” *IEEE Transactions and Propagation*, vol. 53, no. 12, pp. 3870–3876, Dec. 2005.
- [3] International Organization for Standards, “Information technology – radio frequency identification for item management – part 6: Parameters for air interface communications at 860 MHz to 960 MHz,” ISO/IEC, Tech. Rep. 18000-6:2004/Amd 1:2006, 2006.
- [4] D. M. Dobkin and S. Weigand, “Environmental effects on RFID tag antennas,” in *IEEE MTT-S International Microwave Symposium*, Long Beach, CA, June 2005, pp. 4–7.
- [5] D. M. Dobkin, *The RF in RFID: Passive UHF RFID in Practice*. Burlington, MA: Newnes, 2007.
- [6] K. Kurokawa, “Power waves and the scattering matrix,” *IEEE Transactions on Microwave Theory and Technique*, vol. 13, no. 3, pp. 194–202, Mar. 1965.
- [7] T. C. Chau, B. A. Welt, and W. R. Eisentadt, “Analysis and characterization of transponder antennae for radio frequency identification (RFID) systems,” *Packaging Technology and Science*, vol. 19, pp. 33–44, 2006.
- [8] C. Cho and H. C. and, “Broadband RFID tag antenna with quasi-isotropic radiation pattern,” *IEE Electronics Letters*, vol. 41, no. 20, pp. 1091–1092, 2005.
- [9] C. C. Chang and Y. C. Lo, “Broadband RFID tag antenna with capacitively coupled structure,” *Electronics Letters*, vol. 42, no. 23, pp. 1322–1323, Nov. 2006.
- [10] H. W. Son and C. S. Pyo, “Design of RFID tag antennas using an inductively coupled feed,” *IEE Electronics Letters*, vol. 41, no. 18, pp. 994–996, Sept. 2005.
- [11] Alien Technology, “Higgs-3 product overview,” July 2008.
- [12] ST Microelectronics, “XRA00,” Dec. 2004.
- [13] T. G. Tang, Q. M. Tieng, and M. W. Gunn, “Equivalent circuit of a dipole antenna using frequency-independent lumped elements,” *IEEE Transactions on Antennas and Propagation*, vol. 41, no. 1, pp. 100–103, Jan. 1993.
- [14] S. D. Stearns, “Antenna impedance models,” in *ARRL Pacifcon*, ser. Antenna Forum Digest, San Ramon, CA, Oct. 2004, pp. 147–181.
- [15] S. Uda, *Yagi-Uda antenna*. Tohoku University: Research Institute of Electrical Communication, 1954.
- [16] D. B. Miron, *Small Antenna Design*. Burlington, MA: Newnes, 2006.
- [17] F. E. Terman, *Radio Engineer’s Handbook*. New York: McGraw-Hill, 1945.
- [18] P. V. Nikitin and K. V. S. Rao, “Antennas and propagation in UHF RFID systems,” in *Proc. IEEE RFID 2008*, Las Vegas, NV, Apr. 2008.